

Matching the frequency spectrum of PMS stars by means of standard and rotating models

M. Di Criscienzo,¹ P. Ventura,¹ F. D’Antona,¹ M. Marconi,² A. Ruoppo,²
V. Ripepi²

¹*INAF-Osservatorio Astronomico di Roma, via di Frascati 33, 00040, Monteporzio, Roma, Italy*

²*INAF-Osservatorio Astronomico di Capodimonte, via Moiariello 16, 80100, Napoli, Italy*

Accepted ????. Received ??? in original form ??

ABSTRACT

We applied the ATON code to the computation of detailed grids of standard (non-rotating) and rotating Pre-Main Sequence (PMS) models and computed their adiabatic oscillation spectra, with the aim of exploring the seismic properties of young stars. As, until now, only a few frequencies have been determined for ~ 40 PMS stars, the way of approaching the interpretation of the oscillations is not unique. We adopt a method similar to the matching mode method by Guenther and Brown making use, when necessary, also of our rotating evolutionary code to compute the models for PMS stars. The method is described by a preliminary application to the frequency spectrum of two PMS stars (85 and 278) in the young open cluster NGC 6530. For the Star 85 we confirm, with self-consistent rotating models, previous interpretation of the data, attributing three close frequencies to the mode $n=4, l=1$ and $m=0, +1, -1$. For the Star 278 we find a different fit for the frequencies, corresponding to a model within the original error box of the star, and dispute the possibility that this star has a T_{eff} much cooler than the red boundary of the radial instability strip.

Key words: stars: oscillations – stars: evolution – stars: rotation – stars: variable: other – stars: pre-main-sequence

1 INTRODUCTION

The existence of pulsating stars among intermediate mass Herbig Ae/Be stars ($1.5 \lesssim M/M_{\odot} \lesssim 4$) was originally suggested by Breger (1972) and confirmed by the pulsation of HR 5999 (Kurtz & Muller 1999) and HD 104237 (Donati et al. 1997). Considering that young PMS stars like the Herbig Ae/Be stars evolve through the instability region of post-main sequence stars, Marconi & Palla (1998) studied the radial pulsating properties of young stars, defining their instability strip (IS) for radial pulsations. Following work focused also on the search of further candidates, and today several objects have been found and are discussed in the astronomical literature (Marconi et al. 2004; Ripepi et al. 2006a; Zwintz 2008). Most of these stars have more than one pulsation frequency, they look like PMS counterparts of the main sequence (MS) or early post-MS variables of the δ Scuti type. It is now established that the PMS variables can also pulsate in non radial p-modes (Ripepi et al. 2006b, 2007; Zwintz, Guenther & Weiss 2007). Unfortunately, not many frequencies are identified in observations made from the ground, and their analysis then lacks firm identification of modes. Nevertheless, new observations are beginning to be available and more are expected from the program of cur-

rent (COROT) and up coming (KEPLER) space missions. To complicate the things these stars have inherited an angular momentum from the previous protostellar phase, which explains why most of these stars rotate. Recently, the efforts to measure stellar rotation periods — or at least the projected rotational velocities $v \sin i$ — for many stars of different type have been intensified (Royer et al. 2002a,b). In particular projected rotational velocities in very young cluster stars have been measured (Herbst et al. 2005; Petit et al. 2002) with the aim of providing constraints in the modelling of the evolution of angular momentum during the very early phases of stars formation and PMS stages. In particular the study of rotational velocity in the Orion complex (Wolff et al. 2004) has shown that their variation with the evolutionary phase, from the convective PMS to the Main Sequence, is compatible only with decoupling of core and envelope rotation when the stars begin evolving along the radiative tracks.

Since the stellar structure is significantly modified by rotation, rotation will affect not only the age and mass of the star derived from the location in the HR diagram, but also the determination of its physical parameters and of oscillation frequencies in particular. Till now the mode identification,

that is the determination of radial order and spherical harmonic of the observed oscillation spectra, has been based on non rotating evolutionary models for the computation of theoretical frequencies, in some cases only noticing that the observations present a split, probably due to the rotation. As more and more new data from ground and space based observations are likely to become available in the near future, we decided to begin developing theoretical tools for the interpretation of the PMS variability, by using standard and rotating PMS models computed with the code ATON (Ventura et al. 1998; Mendes et al. 1999), and deriving their seismic properties by means of the adiabatic oscillation code LOSC (Scuflaire et al. 2007). In Section 2 we discuss our theoretical tools: the input physics of the models, and the frequency computation. The method adopted for comparing observed and theoretical frequencies is described in Section 3. We test the method, in Section 4, on Star 85 of NGC 6530, and compare our results with those of Guenther et al. (2007) (hereafter G07). We find that rotating models are consistent with the hypothesis of the split in a triplet of the frequency at $180.26 \mu\text{Hz}$. In Section 5, we also discuss the comparison with Star 278 of NGC 6530 whereas in Section 6 we summarize the main findings of this paper.

2 THEORETICAL TOOLS

2.1 The evolutionary code

To build the grids of models we have used the code ATON (Ventura et al. 1998) in its standard version for asteroseismic applications (D’Antona et al. 2005) and in its rotational version, including stellar rotation according to the formulation by Endal & Sofia (1976) as described in Mendes et al. (1999) and in Landin et al. (2006). The program has been recently updated (Ventura, D’Antona & Mazzitelli 2007), and we describe in the following its main physical and numerical inputs.

2.1.1 Input micro-physics

The radiative opacities are taken from Iglesias & Rogers (1997), and extended by the Ferguson et al. (2005) tables in the low temperature ($T \leq 10000$ K) regime; the conductive opacities, harmonically added to the radiative opacities, are taken from Poteckhin (2006, see WEB page www.ioffe.rssi.ru/astro/conduct/). The OPAL equation of state of Rogers et al. (1996), overwritten in the pressure ionization regime by the EOS by Saumon et al. (1995), is used. The EOS is extended to the high-density, high-temperature domain according to the treatment by Stolzmann & Blöcker (2000). A detailed description of the EOS will be presented elsewhere (Ventura & Mazzitelli, in preparation).

2.1.2 Convection treatment

The convective regions can be described either by the traditional Mixing Length Theory (MLT) approach (Bohm-Vitense 1958), or following the Full Spectrum of Turbulence (FST) (Canuto et al. 1996) prescription. All the models presented in this paper have been calculated using the FST treatment. Since this work is focused on PMS

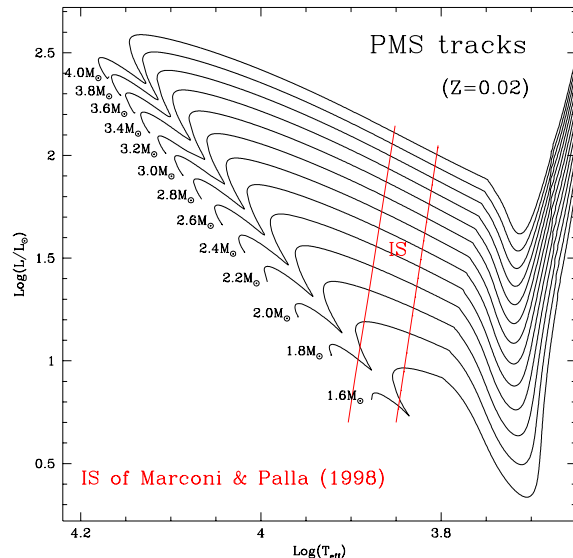


Figure 1. Theoretical HR diagram for the PMS evolution phase. Evolutionary tracks calculated by ATON for the labelled masses are reported. Overplotted is the IS computed by Marconi & Palla (1998).

evolution, no extra-mixing was considered, though the code presents the possibility of allowing some extra-mixing (both in the instantaneous and the diffusive modality) from any convective border.

2.1.3 Chemical composition

All the models were computed with the Grevesse & Noels (1993) solar mixture of heavy elements, and the mass fraction of (X,Y,Z) is (0.70,0.28, 0.02). The initial mass fraction of Deuterium is $X(D) \sim 2 \cdot 10^{-5}$.

2.1.4 Rotation

Rotation was modelled according to the treatment by Endal & Sofia (1976). This approach accounts only for the hydrostatic effects of rotation, neglecting the internal angular momentum redistribution. Three rotation schemes are currently implemented in the code, namely i) rigid rotation of the whole star, ii) local angular momentum conservation everywhere, iii) local angular momentum conservation in the radiative regions and rigid rotation of the convective zones. The initial total angular momentum of the star is provided as a physical input. In this work we used the iii) option in agreement with the analyses of Wolff et al. (2004). The initial angular momentum is chosen to reproduce the observed surface angular velocity of the star at a given position in the HR diagram.

2.2 The model grids

Fig. 1 shows a selected set of our evolutionary tracks from 1.6 to $4 M_{\odot}$ and the radial IS found by Marconi & Palla (1998) for the first three radial modes. In detail it represents

the instability strip limits between the second overtone blue edge and the fundamental red edge. The red edges for non radial oscillations all lie at T_{eff} larger than this, so the fundamental red edge represents the lower effective temperature for any kind of PMS oscillation (Unno et al. 1989). This limit, however, depends on the efficiency of convective treatment, being cooler for a smaller efficiency of convection, as the interaction with deep convection quenches pulsations. The red edge of the radial IS of Marconi & Palla (1998) was obtained with $1/H_p=1.5$ that reproduces the solar radius in their models. Decreasing the mixing length parameter from 1.5 to 1, the red edge becomes cooler by 200K (Marconi & Palla, private communication). Models were computed from 1.5 to 4 M_{\odot} with a step $\Delta M=0.02 M_{\odot}$. The evolution begins in the Hayashi track, and the calculation ends when the star has reached the Main-Sequence. We memorize the structural quantities needed to perform the computation of the oscillation spectrum. The step in effective temperature of this grid is $\Delta T_{\text{eff}} \sim 50\text{K}$. For rotating models we follow a different approach. As the moment of inertia of the model changes along the evolution, together with the total radius and the internal mass distribution also the angular and surface velocity change along the PMS track, increasing from the youngest model (at the lowest examined T_{eff}) to the oldest model (at the hottest T_{eff}). We build up a sub-grid of rotating models after having compared observed frequencies with those of the non rotating grid and having extracted an initial list of best fit models.

2.3 Adiabatic oscillation code

We use the LOSC oscillation code by Scuflaire et al. (2007) to calculate the frequencies of radial and non radial oscillation modes for each grid point. We limit the spherical degree to $l=1,2,3,4$ and cover the interval in angular frequencies between 0.6 and 60 times the dynamical time¹. All these oscillations are computed with the standard surface boundary condition $\delta P/P + (4 + \omega^2)\delta r/r = 0$, where $\omega = 2\pi f \tau_{\text{dyn}}$ is the dimensionless angular frequency.

Beyond the radial order n and the degree l another number characterizes the stellar oscillation frequencies $f_{n,l,m}$: the azimuthal order $m \in [-l, l]$. The rotation breaks the azimuthal symmetry and removes the $2l+1$ degeneracy in m .

In our modelling, we consider the symmetrical part of the centrifugal distortion directly in the computation of rotating stellar models. Then we take into account the first term of perturbation. The perturbation method at the first order² in the rotational velocity Ω predicts an equidistant frequency

splitting $\delta_{l,n}$ between consecutive m components within each (l,n) multiplet, i.e:

$$f_{l,n,m} = f_{l,n,0} + m\beta_{l,n}\Omega/2\pi \quad (1)$$

where β , the coefficient of the rotational splitting, is calculated directly by LOSC for each model. We stress that, as a novelty in the present computation, $f_{l,n,0}$ is the eigenfrequency of (l,n) mode of the stellar rotating model, structure of which depends on the rotation rate.

In Fig. 2 we show how these frequencies change for a model of the same mass ($=2.40M_{\odot}$) and effective temperature ($\sim 7140\text{K}$) but with three different values of equatorial velocity of rotation ($v=0$ (NULL), $v \sim 50$ km/s (INT) and $v \sim 80$ km/s (HIGH)); the figure shows the percentage variations of frequencies with $l=0,1,2$ and $n \leq 26$. The general trend is that the differences increase when the rotation velocity increases. It is interesting to note that for $n > 3-4$ the frequencies of the rotating stars are smaller than those computed for non-rotating models ($<0.2\%$ in the INT case and $<1\%$ for HIGH rotation velocities). For small n , on the contrary, the oscillation frequencies of the rotating models are larger than the non rotating ones, up to 2-3%, although the percentual differences globally decrease for increasing n . We see that there is some scatter in the points at low n (see, e.g., the scatter in dots and triangles at $n = 6,7,8$). This is part of the problem appearing in the computation of frequencies for small n in the LOSC code. The problem will be carefully investigated in the near future, as PMS stars oscillate mainly at this low n modes.

3 COMPARING OBSERVED AND PREDICTED FREQUENCIES: THE METHOD

The methodology that we will adopt to model the sparse radial and non-radial oscillation spectra observed in pulsating PMS stars was originally suggested and developed by Guenther & Brown (2004) and used recently by G07 to model the oscillations of five pulsating stars in NGC 6530. As recently reviewed by Cunha et al. (2007), there are several other methods for mode identification of the frequencies that constitute the observed spectra of a given star and/or to constrain the mass and age of this star. These methods use at the same time radial and non radial frequencies. Among them, one of the most popular consists in the use of the asymptotic theory and of the large and small separation in particular (Ruoppo et al. 2007). This is a good strategy if the star oscillates in the asymptotic regime, or when the oscillation data are not well determined but, for the higher quality data expected from satellites, e.g. from COROT, a more flexible choice is to use all the diagnostic informations obtained from the data, and in particular all the discovered frequencies (Guenther & Brown 2004).

Indeed, direct fitting of the frequencies is a relatively simple way to find a good first solution to the problem of mode identification, and this will become an ever and ever better tool with higher quality data. In principle, one could proceed with seismic modelling comparing all values for (l, n) to each of the detected frequencies. The value of degree l is

¹ $\tau_{\text{dyn}} = \sqrt{\frac{R^3}{GM}}$

² In fact recently, Lovekin & Deupree (2008) using detailed 2D stellar models and a 2D finite difference integration of the linearized pulsation equations to compute non radial oscillations have definitively demonstrated that the eigenfunction can be accurately modelled using the perturbation theory and a single spherical harmonic, if rotation is slow enough ($v_{\text{eq}} \lesssim 90$ km/s). For these velocities is justified to neglect perturbation orders greater than one.

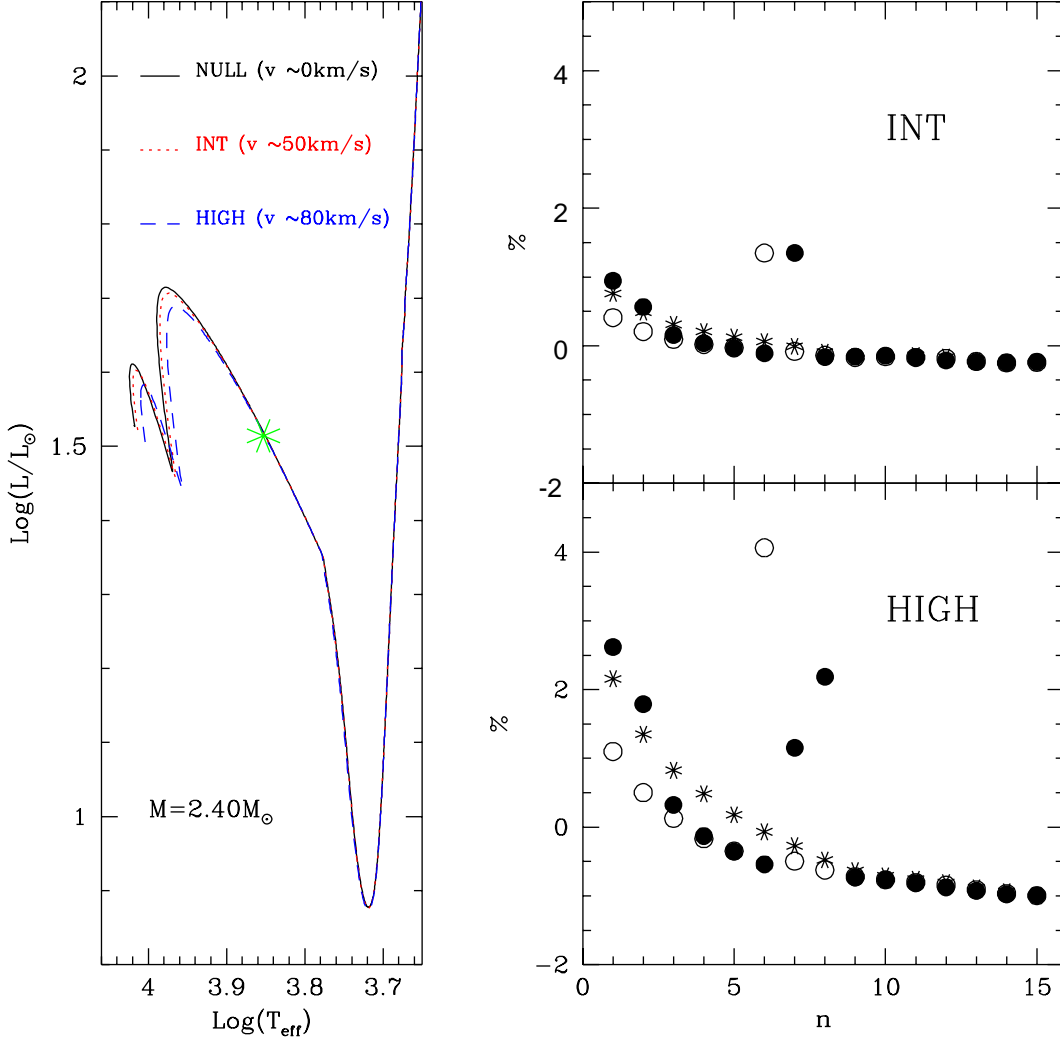


Figure 2. *Left panel:* PMS tracks corresponding to $M=2.4 M_\odot$ and computed with different rotation velocities (see text). *Right panels:* differences (in percentage) for each pair of n and l (0-asterisk, 1-open dots, 2-filled dots) between frequencies of rotating models and NULL ones for the models labelled with an asterisk in left panel.

usually limited ($l \leq 4$)³ and $m=0$ is assumed when no obvious evidence of rotational splitting is present in the observed spectrum. Given the N frequencies of a particular star, into our grid of the oscillation spectra we look for models having $\chi^2 \leq 1$, where:

$$\chi^2 = \frac{1}{N} \sum_{i=1}^N \frac{(\nu_{\text{obs},i} - \nu_{\text{mod},i})^2}{\sigma_{\text{obs},i}^2 + \sigma_{\text{mod},i}^2} \quad (2)$$

$\nu_{\text{obs},i}$ and $\nu_{\text{mod},i}$ are respectively the observed frequency and the corresponding model frequency for the i th frequency,

$\sigma_{\text{obs},i}^2$ and $\sigma_{\text{mod},i}^2$ the associated uncertainties⁴. In general the search for the best-fit model (which has the spectrum that minimizes the χ^2) is done only in a sub-grid made of models within the 3σ error box in T_{eff} and L of the star. If the program does not find any models with $\chi^2 \leq 1$, that means that not all frequencies are matched within the errors, it discards one by one the non-matched frequencies, computes again the χ^2 for the remaining frequencies and searches again for models with $\chi^2 \leq 1$. The models with the lower value of the χ^2 is the best-fit model.

When possible, we use the observed frequencies according to the order with which they are extracted from the Fourier

³ This consideration is based on a geometric statement. In fact in distant stars, only the large scale structures can be detected and the sensitivity of brightness variations is restricted to modes up to 3 or 4 node lines at the surface.

⁴ For the available observations the model uncertainties are negligible, as they are an order of magnitude smaller than the observational ones (see Guenher & Brown, 2004 for a discussion on this topic)

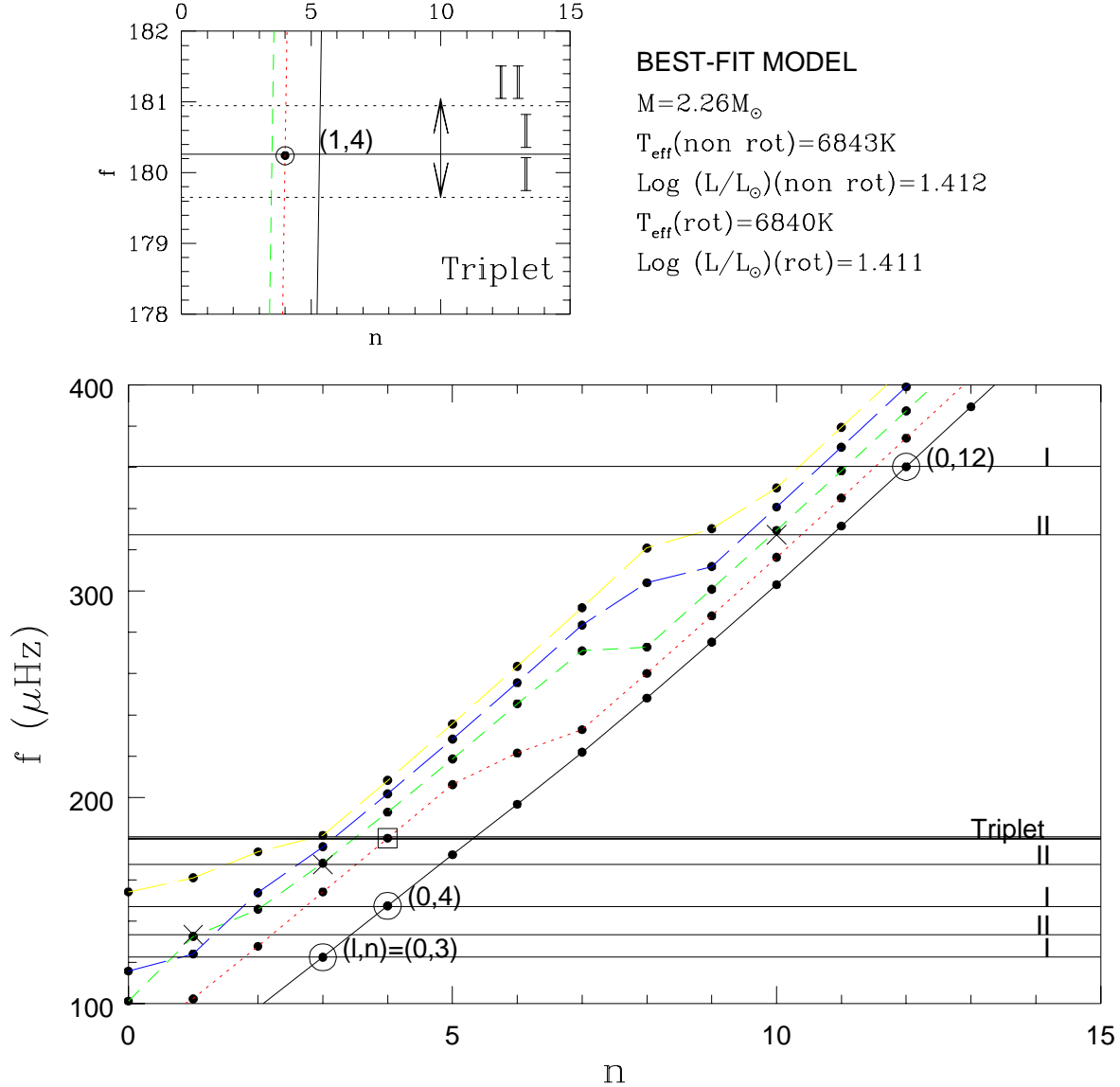


Figure 4. Comparison between the observed spectrum of Star 85 and the spectrum of the best fit model (filled triangle in Fig. 3). Solid, dotted, dashed and long dashed lines connect theoretical frequencies with respectively $l=0, 1, 2, 3, 4$. In the small box we report a zoom around the frequency $180.26 \mu\text{Hz}$ in order to underline the split due to the rotation of the star.

our best-fit models. This box is larger than those used by G07 as we have noticed that their best-fit model lies just on the cool edge of the observational box. Only three models fit within the errors all four⁷ frequencies ($\chi^2 \leq 1$). In Fig. 3 we report these models with triangles; the filled one is that with the lowest value of χ^2 , i.e. our best fit model which is practically overlapped to the model of G07 (filled circle). Also the mode identification is the same, with the three frequencies f_2, f_4, f_5 matched with $(l,n)=(0,4), (0,3), (0,12)$, and the splitted one (f_1) with $(l,n)=(1,4)$ (see Fig. 4).

Alternatively, by fixing these four pairs of (l,n) to the ob-

served frequencies, the models with the lowest χ^2 (including the three ones previously found) all lie on a diagonal of HR diagram (see Fig. 3) as found for the case B by G07. This can be understood in the following way: by choosing these pairs (l,n) we assign a large separation ($= f_{n,l} - f_{n-1,l}$), which in asymptotic regime depends linearly on luminosity and temperature as shown by Ruoppo et al. (2007).

Concluding, using similar hypotheses, we obtain the same result of G07, i.e. the same best-fit model. The same models are selected, when we search among all the grid models. Adding the frequencies found during the recheck of the data doesn't change the model with lowest χ^2 but in this case the lowest χ^2 is not ≤ 1 . Looking in detail to the comparison, the main reason for this is that the three new frequen-

⁷ We have discarded f_3 which is a splittet frequency.

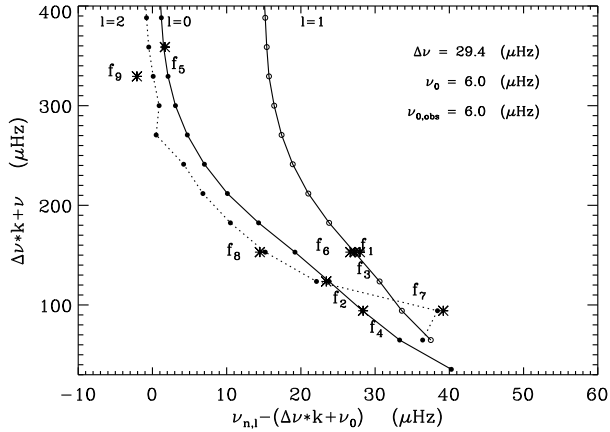


Figure 5. Echelle diagram for star 85, using the theoretical frequencies of the best fit model shown in Fig. 4. The parameters used to reproduce this plot are also shown.

cies (f7, f8 and f9 in particular) are not perfectly matched ($\Delta f > \sigma_{obs}$ from the nearest ones with $l=2$). This problem was also found in the G07 investigation. A possible interpretation is given in the next subsection.

4.2 The second step: rotating models

Now we implement the comparison with rotating evolutionary models. Using the observed splitting $\Delta f = 0.643 \pm 0.09 \mu\text{Hz}$ ($= \frac{f_6 - f_3}{2}$), Eq. 1 and the radius of the best-fit model found in the previous section we derive a rotation rate of $v_{eq} \sim 10 \text{ km/s}$. We calculated a sub-grid of rotating models choosing an initial angular momentum that allows to obtain the predicted velocity near the position in HR diagram of the best-fit model previously found.

The model grid is restricted to $2 \leq \frac{M}{M_{\odot}} \leq 2.5$ and has the same step in T_{eff} and mass of the non-rotational grid. The rotational velocity is $v_{eq} \sim 10 \text{ km/s}$ around $\log T_{eff} = 3.83$. We compared again observed and calculated spectra looking for a good match in terms of χ^2 . Such a slow rotation velocity modifies very little both the structure of the star and its position in HR diagram, so we obtain identical results. Although we find the same three best fit models by considering the fit of the first frequencies only, when we add the three additional frequencies the rotating models match them better but continues to lie 1σ away from the nearest theoretical frequency. Maybe it would be useful to recheck the data of the second round. An alternative explanation for this discrepancy is the following. Daszynska-Daszkiewicz et al. (2002) tested the results of non adiabatic models on the β Cep stars. One of the effects of an even slow rotation, is to influence mode properties, when there is a small frequency distance between modes with the same azimuthal order m and spherical harmonic degree l differing by 2. In this case each of the coupled modes must be represented by a certain superposition of spherical harmonics of the two models involved. This effect was invoked to explain the nonradial character of pulsation in β Cep stars but it could be a possible motivation for the worse match of the three last frequencies, either with the closest frequencies with $l=2$, or with those with $l=0$. It

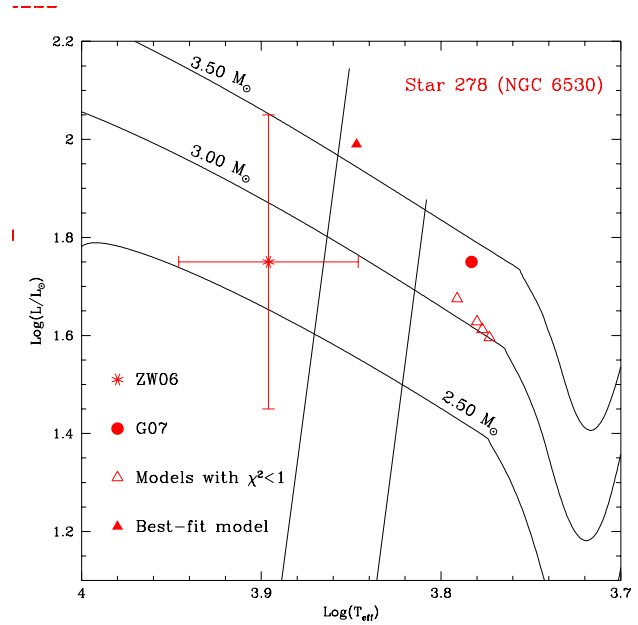


Figure 6. The position of Star 278 in the HR diagram (see text). Solid lines are evolutionary tracks calculated with the ATON code with no rotation.

Table 2. Observed frequencies of Star 278. In the third and fourth column we have reported the l and n identification of the best fit model obtained searching inside the observational box. With asterisks are labelled those frequencies which are not matched. For this frequencies we report l and n of the nearest frequency ($\Delta f_2 \sim 1.3 \mu\text{Hz}$ and $\Delta f_7 \sim 0.8 \mu\text{Hz}$)

No.	Frequency	l	n
f1	83.3	2	3
f2	140.3	0*	9*
f3	187.7	3	11
f4	48.3	0	2
f5	109.8	2	6
f6	69.6	4	3
f7	138.7	2*	8*
f8	181.5	2	11
f9	160.8	1	10

is important to stress that this is only a suggestion and that a definitive statement will be possible only when better data will be available.

5 EXAMPLE-2: STAR 278 OF NGC 6530

Now we analyze Star 278 in NGC 6530. Among the nine frequencies emerged from the Fourier analysis of the data performed by ZW07, G07 were able to fit all with $l=0,1,2$ p modes, except the lowest one. All their best fit models lie at a much lower T_{eff} (1800K below the mean temperature given by ZW06). The authors support this interpretation considering that this star, together with some other stars in the cluster, might have been dereddened in excess in ZW06, when their color temperatures were derived. To support this

hypothesis, they notice that the amount of gas near these stars correlates linearly with the difference between model and observed surface temperature.

This T_{eff} is really very low, if compared to the red edge of the IS calculated by Marconi & Palla (1998) ($\sim 600\text{K}$ see Fig. 6). As pointed out in Section 3 the cool edge of the radial IS also applies to non radial oscillations, and it only depends on the efficiency of convective treatment, being cooler for a smaller efficiency of convection. In particular, the red edge of the radial IS of Marconi & Palla (1998) was obtained with a value of $l/H_p=1.5$ and its effective temperature decreases by $\sim 200\text{ K}$ for $l/H_p=1$ remaining still hotter than the best fit of G07. The efficiency of convection in pre-MS can be tested for the convective Hayashi phase of the low mass stars by using the location in the HR diagram of pre-MS binaries. The binaries however do not provide a calibration for the stars located on the 'radiative' phase of the tracks, which is practically independent on the convection model. In fact, the analysis of dynamical PMS masses shows a good agreement with all stellar models for $M \geq 1.2 M_{\odot}$ (Hillenbrand & White 2004) for which there are no stars on the convective tracks in the examined sample. We know that at the solar T_{eff} (5780K) the l/H_p ratio must be quite large for models to fit the solar radius. We also have further hints for models at larger T_{eff} , where the convective layer becomes very thin. Non local models of convection (Kupka & Montgomery 2002) for A stars between 7200 and 8500 K can not be easily compared to MLT results, but comparable values of the maximum convective flux in the H-convection zone are obtained with $\alpha=1$ at $T_{\text{eff}} \sim 7100\text{K}$ ($\log T_{\text{eff}}=3.85$) and with $\alpha=0.4$ at $T_{\text{eff}} \sim 8000\text{K}$ ($\log T_{\text{eff}}=3.90$). Thus non local models shows that the convection efficiency is much smaller than in standard MLT models at the blue boundary of the IS, but rapidly increase while convection deepens. It is clear that a further exam of the IS boundaries is needed. For the present test we prefer to search in the observational box allowing only temperatures hotter than the IS red edge obtained by Marconi & Palla (1998).

We have studied this star using our grid of non rotating models since no evidence of relevant rotation is observed in the spectrum. This does not mean that the star does not rotate, but it could mean that the star rotates so slow that the effect on the frequencies is smaller than the observational uncertainties. Using the luminosity and temperature given by ZW06 and the same size of the observational box used for Star 85 we are able to reproduce only seven of the nine frequencies. It is important to say that among the models able to reproduce seven frequencies only one model in the grid has $\chi^2 < 1$: the position of this best fit model in the HR diagram is reported in Fig. 6 and the mode identification in Table 2. The only non matched frequencies are those two which lie very close to each other. As we noticed discussing the results for Star 85 also in this case the theoretical frequencies which are close to these two observed ones have l that differs by 2 (see rows marked with asterisks in Table 2) and they may emerge in the observed spectra as coupled modes due to the rotation, even if slow enough that we don't see it as split of frequencies with $l \neq 0$, as suggested Daszynska-Daszkiewicz et al. (2002). But a definitive conclusion can be done only when new data will be available. In this direction also goes the observation that the two frequencies that we are not able to match with the theo-

retical ones are so close, suggesting the presence of a third one, that could be a part of a triplet due to the rotation. Unfortunately, is impossible to find this frequency from the available data.

6 CONCLUSIONS

In this paper we have discussed the potentialities of a method built up for the interpretation of the observed multi-frequency spectra of pulsating stars, giving us the possibility of constraining its mass and age.

The method relies on the direct comparison of the observed oscillation spectrum of a given star with a database of theoretical ones. How well a given theoretical spectrum matches with the observed one is measured by χ^2 . Each frequency set in the database was computed using the LOSC adiabatic oscillation code to derive the pulsation frequencies of the evolutionary models computed with the ATON code. The characteristics of the grid were reported in Section 3 and it is fine enough to determine a best fit model to the oscillation data as constrained solely by observed frequencies. Till now, the method has been applied only to the interpretation of the PMS pulsating stars, but the intention is to extend it also to later evolutionary phases.

We have included the rotation of the star not only considering the removal of the m -degeneracy, but also in the calculation of the evolutionary models from which we compute the pulsational frequencies. During the evolution, the angular momentum distribution assumes rigid rotation in the convective layers, and conservation of the momentum shell by shell, in the radiative core, as suggested by Wolff et al. (2004). We have shown that, for the some physical inputs, the variations of frequencies with rotation are small but significative especially when better data will come, from current space missions for example. In particular, our calculations have demonstrated that the differences increase when the rotation velocity increases. While the frequencies of the rotating stars are smaller than those computed for non-rotating models for $n > 5-6$, inversely for small n the oscillation frequencies of the rotating models are larger then the non rotating ones, up to 2-3% for stars that rotate with $v_{\text{eq}} \sim 80\text{ km/s}$.

We have tested the mode-matching method on data of two stars of NGC 6530. For the Star 85 we confirm with self-consistent rotating models the interpretation of the data performed by G07, attributing three close frequencies to the mode $n=4, l=1$ and $m=0, +1, -1$. We also found that the remaining three frequencies are better matched when rotating models are used. For the Star 278 we find a different fit for the frequencies, corresponding to a model within the original error box of the star, and dispute the possibility that this star has a T_{eff} much cooler that the red boundary of the radial instability strip published by Marconi & Palla (1998).

ACKNOWLEDGMENTS

It is a pleasure to thank R. Scuflaire and J. Montalbán for having provided us the Liège Oscillation Code (LOSC) and the referee W. W. Weiss for his useful suggestions that

improved the final version of the paper.

Financial support for this study was provided by MIUR under the PRIN project “Asteroseismology: a necessary tool for the advancement in the study of stellar structure, dynamics and evolution”, P.I. L. Paternó.

REFERENCES

- Bohm-Vitense, E. 1958, *Z. Astroph.*, 46, 108
- Breger, M. 1972, *ApJ*, 171, 539
- Canuto, V. M., Goldman, I., & Mazzitelli, I. 1996, *ApJ*, 473, 570
- Cunha et al. 2007, &ARv, 14, 217
- Daszynska-Daszkiewicz, J., Dziembowski, W. A., Pamyatnykh, A. A., & Goupil, M.-J. 2002, *A&A*, 392, 151
- Kurtz, D. W., & Marang, F. 1995, *MNRAS*, 276, 191
- Donati, J.-F., Semel, M., Carter, B. D., Rees, D. E., & Cameron, A. C. 1997, *MNRAS*, 291, 658
- D’Antona, F., Cardini, D., Di Mauro, M. P., Maceroni, C., Mazzitelli, I., & Montalbán, J. 2005, *MNRAS*, 363, 847
- Endal, A. S., & Sofia, S. 1976, *ApJ*, 210, 184
- Ferguson, J. W., Alexander, D. R., Allard, F., et al. 2005, *ApJ*, 623, 585
- Grevesse, N., & Noels, A. 1993, in *Origin and Evolution of the Elements*, ed. N. Pratz, E. Vangioni-Flam, & M. Casse (Cambridge Univ. Press), 15
- Guenther, D. B. & Brown, K. I. T. 2004, *ApJ*, 600, 419
- Guenther, D. B., Kallinger, T., Zwintz, K., Weiss, W. W., & Tanner, J. 2007, *ApJ*, 671, 581 (G07)
- Herbst, W., Mundt, R. 2005, *ApJ*, 633, 967H
- Hillenbrand, L. A. & White, R. J., 2004, *ApJ*, 604, 741
- Iglesias, C. A., & Rogers, F. J. 1996, *ApJ*, 464, 943
- N. R. Landin, P. Ventura, F. D’Antona, L. T. S. Mendes, L. P. R. Vaz, 2006, 456, 269
- Lovekin, C. & Deupree, R., 2008, *ApJ*, in press (arXiv:0803.2053)
- Marconi, M., & Palla, F. 1998, *ApJ*, 507, L141
- Marconi, M., Ripepi, V., Palla, F., & Ruoppo, A. 2004, *CoAst*, 145, 61
- Mendes, L. T. S., D’Antona, F., & Mazzitelli, I. 1999, *A&A*, 341, 174
- Petit P., Donati J.-F., Cameron A., 2002, *MNRAS*, 334, 374
- Ripepi, V., Marconi, M., Palla, F., Bernabei, S., Ruoppo, A., Cusano, F., Alcal, J. M., 2006a, *MmSAI*, 77, 317
- Ripepi, V., Bernabei, S., Marconi, M., Palla, F., Arellano Ferro, A., Bonanno, A., Ferrara, P., Frasca, A., Jiang, X. J., Kim, S.-L. et al. 2006b, *A&A*, 449, 335
- Ripepi, V., Bernabei, S., Marconi, M., Ruoppo, A., Palla, F., Monteiro, M. J. P. F. G., Marques, J. P., Ferrara, P., Marinoni, S., Terranegra, L. 2007, *A&A*, 462, 1023
- Rogers, F. J., Swenson, F. J., & Iglesias, C. A. 1996, *ApJ*, 456, 902
- Royer, F., Gerbaldi, M., Faraggiana, R., Gmez, A. E., 2002, *A&A*, 381, 105(a)
- Royer F., Grenier S., Baylac M.-O., Gmez A. E., Zorec J., 2002, *A&A*, 393, 897(b)
- Ruoppo, A., Marconi, M., Marques, J. P., Monteiro, M. J. P. F. G., Christensen-Dalsgaard, J., Palla, F., Ripepi, V. 2007 *A&A*, 466, 261R
- Saumon, D., Chabrier, G., Van Horn, H. M., 1995, *ApJs*, 99, 713
- Scuflaire, R., Montalbán, J., Theado, S., Bourge, P.-O., Miglio, A., Godart, M., Thoul, A., Noels, A., 2007, (arXiv:0712.3474)
- Stolzmann, W. & Blöcker, T., 2000, *A*, 361, 1152
- Treu, T. et al., 2003, *ApJ*, 591, 53
- Unno, W., Osaki, Y., Ando, H., & Shibahashi, H. 1979, *Nonradial Oscillations of Stars*, (University of Tokyo Press)
- Wolff, S. C., Strom, S. E., & Hillenbrand, L. A. 2004, *ApJ*, 601, 979
- Ventura, P., Zeppieri, A. D’Antona, A., Mazzitelli, I., 1998, *A*, 334, 953
- Ventura, P., D’Antona, F., & Mazzitelli, I. 2007, *Ap&SS*, 420
- Zwintz, K., & Weiss, W. W. 2006, *A&A*, 457, 237 (ZW06)
- Zwintz, K. 2008, *ApJ*, 673, 1088
- Zwintz, K., Guenther, D. B., & Weiss, W. W. 2007, *ApJ*, 655, 342